20th-century strain accumulation on the Lesser Antilles megathrust based on coral microatolls

Belle Philibosian [a,b,*], Nathalie Feuillet [a], Jennifer Weil-Accardo [a,c], Eric Jacques [a], Abel Guihou [c], Anne-Sophie Mériaux [d,e], André Anglade [f,g], Jean-Marie Saurel [a], Sébastien Deroussi [f]

[a] Université de Paris, Institut de physique du globe de Paris, CNRS, F-75005 Paris, France
[b] U.S. Geological Survey Earthquake Science Center, P.O. Box 158, Moffett Field, CA, 94035, United States of America [1]
[c] Centre Européen de Recherche et d'Enseignement des Géosciences de l'Environnement (CEREGE), Aix-en-Provence, France [2]
[d] School of Geography Politics and Sociology, Newcastle University, Newcastle upon Tyne, NE1 7RU, United Kingdom
[e] Institut Terre Environnement de Strasbourg, UMR 7063 CNRS / Université de Strasbourg, 5, rue René Descartes, 67084 Strasbourg cedex, France [3]
[f] Observatoire Volcanologique et Sismologique de Guadeloupe (OVSG), Institut de Physique du Globe de Paris, France
[g] I3S - CNRS, Université Côte d'Azur, Sophia Antipolis, France [4]

ABSTRACT

The seismic potential of the Lesser Antilles megathrust remains poorly known, despite the potential hazard it poses to numerous island populations and its proximity to the Americas. As it has not produced any large earthquakes in the instrumental era, the megathrust is often assumed to be aseismic. However, historical records of great earthquakes in the 19th century and earlier, which were most likely megathrust ruptures, demonstrate that the subduction is not entirely aseismic. Recent occurrences of giant earthquakes in areas where such events were previously thought to be improbable have illustrated the importance of critically evaluating the seismic potential of other "low-hazard" subduction zones, such as the Lesser Antilles.

Using the method of coral microatoll paleogeodesy developed in Sumatra, we examine 20th-century vertical deformation on the forearc islands of the Lesser Antilles and model the underlying strain accumulation on the megathrust. Our data indicate that the eastern coasts of the forearc islands have been subsiding by up to ∼8 mm/yr relative to sites closer to the arc, suggesting that on the time scale of the 20th century, a portion of the megathrust just east of the forearc islands has been locked. Our findings are in contrast to recent models based on satellite geodesy that suggest little or no strain accumulation anywhere along the Lesser Antilles megathrust. This discrepancy is potentially explained by the different time scales of measurement, as recent studies elsewhere have indicated that interseismic coupling patterns may vary on decadal time scales and that century-scale or longer records are required to fully assess seismic potential. The accumulated strain we have detected will likely be released in future megathrust earthquakes, uplifting previously subsiding areas and potentially causing widespread damage from strong ground motion and tsunami waves.

Published by Elsevier B.V. This is an open access article under the CC BY license (http://creativecommons.org/licenses/by/4.0/).

1. Introduction

1.1. The Lesser Antilles

The Lesser Antilles subduction zone is formed where the oceanic North and South American Plates plunge beneath the Caribbean Plate along the eastern edge of the Caribbean Sea, producing a volcanic arc (Fig. 1). This region has been struck by several large, damaging earthquakes during the historical period, with the largest occurring in the middle of the 19th century. Earthquakes on January 11, 1839 and February 8, 1843 respectively
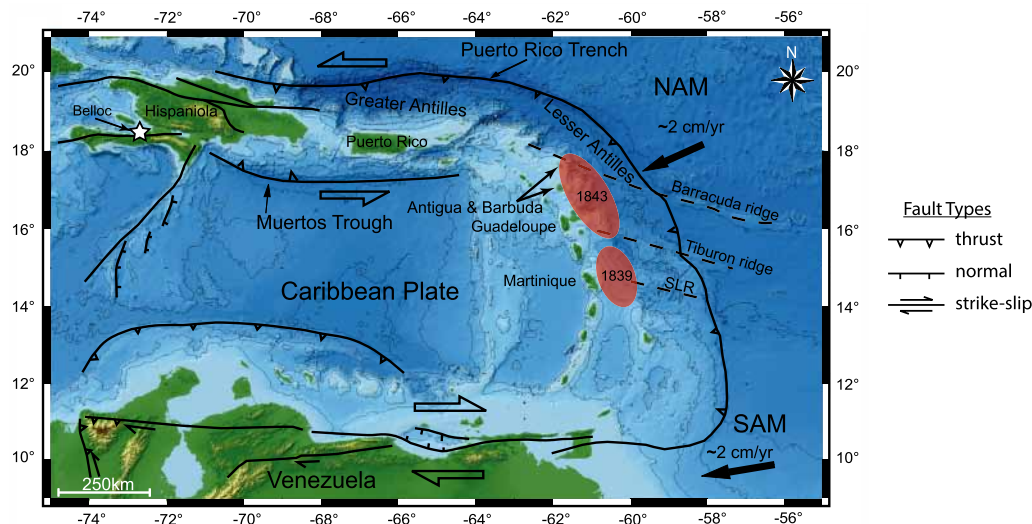
* Corresponding author at: U.S. Geological Survey Earthquake Science Center, P.O. Box 158, Moffett Field, CA, 94035, United States of America.
E-mail address: bphilibosian@usgs.gov (B. Philibosian).
[1] Present address of Belle Philibosian.
[2] Present address of Jennifer Weil-Accardo.
[3] Present address of Anne-Sophie Mériaux.
[4] Present address of André Anglade.

Fig. 1. Regional map with tectonic setting of the Lesser Antilles and estimated rupture areas of 19th-century great earthquakes from Feuillet et al. (2011). Location of coral study site at Belloc, Haiti is marked by a white star. NAM and SAM indicate the North and South American Plates, respectively (the weakly convergent boundary between them is not well defined or expressed east of the Caribbean Plate). SLR: Saint Lucia Ridge.

destroyed the main towns of Fort-Royal (now Fort-de-France) on Martinique Island and Pointe-à-Pitre on Guadeloupe Island and killed over a thousand people (Feuillet et al., 2011). These earthquakes are estimated to have had moment magnitudes between 7.5 and 8.5 and probably occurred on the subduction megathrust interface. Based on previously unconsidered felt reports along the east coast of the United States, Hough (2013) assigned a magnitude of ∼8.5 to the 1843 event. Due to increased population density, it is possible that an earthquake comparable to the 1843 event, occurring today, would kill tens of thousands of people. Furthermore, the megathrust might be capable of rupturing in even larger earthquakes; the ∼200-year-long historical record is far too short to rule out such a possibility. The M_w 9+ 2004 Aceh–Andaman and 2011 Tohoku-oki earthquakes both occurred along subduction zones which, based on historical seismicity catalogs, were previously thought incapable of producing magnitude 9 ruptures, and it is generally unwise to rule out the possibility of such events based on a short historical record or subduction zone characteristics (McCaffrey, 2008). If we utilize geologic records to investigate the past behavior of the Lesser Antilles megathrust and other associated faults beyond short and incomplete historical records, we can properly understand the current seismic and tsunami hazard in the Caribbean region.

1.2. Surface deformation as a key to fault slip

The overriding plate in a subduction zone deforms elastically during the various stages of the seismic cycle due to slip on different parts of the plate interface (Fig. 2). During the interseismic period, stress builds on the shallower, seismogenic portion of the megathrust, which is locked, while the deep plate interface slips aseismically at the rate of plate motion. This causes the area near the trench to subside as it is dragged down by the subducting plate, while the area farther away from the trench is uplifted. When the locked portion of the megathrust ruptures (coseismically), the opposite pattern of deformation occurs. If these two deformation processes are perfectly elastic, the vertical coseismic deformation is expected to exactly cancel the interseismic deformation (e.g., Savage, 1983), whereas splay faulting or distributed plastic deformation within the upper plate will produce permanent deformation.

Measuring the distribution of coseismic and interseismic deformation allows us to infer the underlying behavior on the megath-

rust interface. The area which is locked during the interseismic period is expected to rupture in great earthquakes, so measuring interseismic deformation permits better seismic forecasting. In recent decades these observations can be made very precisely using instrumental geodetic techniques such as measuring the motion of global navigation satellite system (GNSS) stations. However, since the distribution of GNSS stations is generally sparse and covers a geologically short period of time, deformation patterns can be better characterized by using a natural recorder of vertical deformation, coral microatolls.

Weil-Accardo et al. (2016a) pioneered the tectonic study of coral microatolls in the Lesser Antilles, building a 230-year history of vertical deformation on eastern Martinique island. They documented slow subsidence (averaging 1.3 ± 1.3 mm/yr) punctuated by two potentially seismic disturbances: coral transport and changes in deformation rate associated with the 1839 earthquake, and up to 20 cm of subsidence associated with a magnitude ∼7 earthquake in 1946. While Weil-Accardo et al. (2016a) speculated that the subsidence was a result of interseismic locking on the megathrust interface, the rate is very low (not unexpected, since Martinique is quite far from the subduction deformation front) and the inferences that can be drawn from a single study location are limited. In this study, we expand the analysis to a wider distribution of 12 additional sites on Guadeloupe, Antigua, Barbuda, and Anguilla Islands, generally much closer to the deformation front.

2. Coral microatoll paleoseismology & paleogeodesy techniques

Corals with "massive" morphologies begin growth with the attachment of a single polyp to a rocky or sandy substrate. Subsequent growth of the colony (at rates ranging from a few millimeters to a few centimeters per year) is radial, producing an approximately hemispherical shape. Most hemispherical corals also produce annual growth bands similar to tree rings due to seasonal aragonite density variations. In very shallow-water environments, the coral grows upward and outward until it reaches its upward limit of growth, determined by sea level, at which point the portion of the coral exposed above this limit begins to die. This upward limit, above which the degree of exposure becomes fatal, is called the highest level of survival (HLS). Hemispherical corals growing in the intertidal zone develop into "microatolls" when their tops reach HLS, after which their upward growth tracks relative sea level (RSL) while their outward growth continues unim-
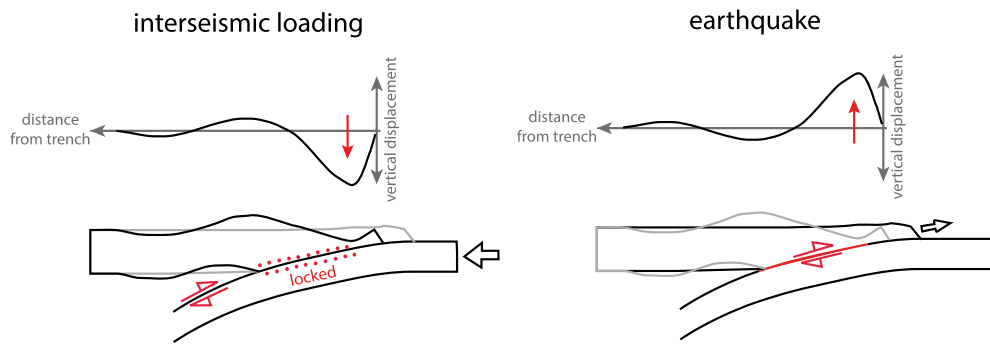
Fig. 2. Schematic diagram of elastic deformation during the interseismic and coseismic phases of a subduction earthquake cycle (after Savage, 1983). Postseismic deformation is more variable, but often includes short-term subsidence in the coseismically uplifted area due to afterslip at the periphery of the rupture area and longer-term low-amplitude regional deformation due to viscoelastic relaxation.
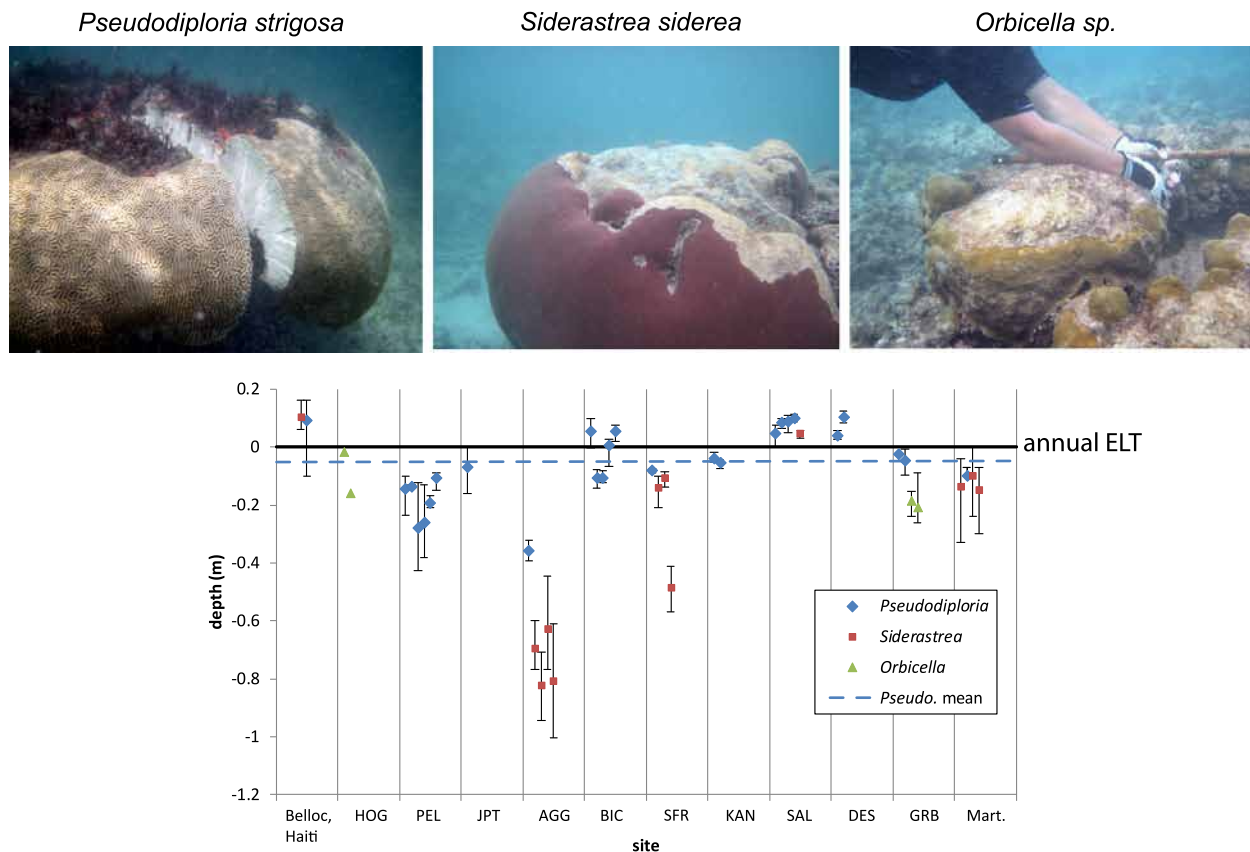

Fig. 3. (top) Examples of microatolls formed from three radially growing coral species. *Pseudodiploria strigosa* (brain coral) was formerly classified as *Diploria strigosa* and genus *Orbicella* as part of genus *Montastrea* (Budd et al., 2012). Genus *Orbicella* contains the three species *O. annularis, franksi,* and *faveolata*, but these are difficult to distinguish in the field. (bottom) Distribution of living coral highest level of survival (HLS) relative to annual extreme low tide (ELT). Each data point represents a single microatoll except at Belloc and Martinique, where each point represents a single site (condensed from Weil-Accardo et al., 2016a, 2016b). Error bars indicate full range of HLS elevation around the mean. JPT indicates Johnson Point, Antigua at 17.024°N, 61.887°W; locations and full names of other sites appear in Table 1. Blue dashed line indicates mean depth of *Pseudodiploria* HLS in the Antigua-Barbuda-Guadeloupe region excluding the anomalously deep specimen at site AGG. (For interpretation of the colors in the figure(s), the reader is referred to the web version of this article.)

peded. The term "microatoll" was coined to describe coral colonies with dead, flat tops and a living outer perimeter. At least three species of Caribbean corals are capable of forming microatolls (Fig. 3).

We measured the depth of living microatoll rims at each site and calculated HLS relative to annual extreme low tide using tide models and satellite altimetry measurements of sea level anomalies (SLA) during the time of our field measurements. Tides for most sites presented in this paper were calculated using the TPXO-Atlas 7.2 global tide model (Egbert and Erofeeva, 2002) in SPOTL

(Agnew, 2012), while those for the Saint-François, Belloc (Haiti), and Martinique sites were calculated using a model from SHOM (Hydrographic and Oceanographic Department of the French Navy) (see Weil-Accardo, 2014; Weil-Accardo et al., 2016a, 2016b). SLA for each location was extracted from the Ssalto/Duacs L4 reprocessed dataset, which is gridded at 0.25° intervals and produced and distributed by the Copernicus Marine and Environment Monitoring Service (CMEMS; http://www.marine.copernicus.eu). HLS for these corals varies somewhat from site to site and specimen to specimen, but generally lies between 10 cm above and 20 cm be-

low the annual extreme low tide (Fig. 3). We include the Belloc, Haiti site for comparison of regional sea-level tracking (location shown on Fig. 1). The consistency of measured HLS relative to sea level within a given site and species confirms that the microatolls are tracking RSL.

Because coral microatolls track RSL, they record tectonic uplift and subsidence, as was originally noted by Taylor et al. (1987). Oceanographic changes are also recorded, but the two sources can typically be distinguished based on time scale and geographic distribution. A radial slice of a microatoll with annual bands allows the reconstruction of a time series of RSL over the lifetime of the coral colony, including the rate of interseismic deformation and the magnitude and timing of coseismic deformation. (Extraction of a slice using a hydraulic chainsaw kills only a small patch of living coral on the outer perimeter of the colony, and surrounding coral has been observed to fill in the gaps after several years' growth if the colony is in good health.) Large coseismic uplifts can raise entire colonies above water, killing them completely. Coral microatolls live for decades or centuries and may be preserved for centuries or millennia after they die, allowing continuous records of vertical deformation to be constructed over long periods of time. This has been done very successfully along the Sunda megathrust in Sumatra (e.g., Meltzner et al., 2015; Philibosian et al., 2017).

3. Data from coral microatolls in the Lesser Antilles

Using aerial imagery and surveys by helicopter and boat between 2006 and 2014, we canvassed the shores of Guadeloupe, Marie-Galante, La Désirade, Antigua, Barbuda, and Anguilla islands for microatolls. It is clear from our search that "fossil" microatolls (those that died in the past) are extremely rare on these islands, and even living microatolls are far less common in the Lesser Antilles than in Sumatra. The living microatolls we found had also commonly been overturned at some point in their lives, and one had even been overturned twice. We hypothesize that hurricane activity may disrupt the long-term preservation of Caribbean microatolls (the Sumatran region is not affected by tropical cyclones). Additionally, the Caribbean coral species are different from those in Indonesia, and their specific skeletal structures may affect long-term preservation. It is also possible that Antillean fossil corals previously existed but have been disturbed or removed by humans for use as building materials. Coral rock is a commonly used building material in both the Sumatran forearc islands and in the Lesser Antilles, but the Antilles have higher human population density. Finally, the continuously rising late Holocene sea level in most of the Caribbean (~0.5 mm/yr in the Lesser Antilles; Khan et al., 2017) may have inhibited the formation of microatolls if coral growth was unable to keep pace, and any older microatolls that did form would now be underwater where they are difficult to find as well as subject to disturbance by waves. In contrast, equatorial regions such as Sumatra generally experienced a mid-Holocene highstand with subsequently stable or falling sea level (e.g., Khan et al., 2015), although the pervasive tectonic deformation inhibits direct measurement of Holocene paleo sea level in Sumatra specifically (Briggs et al., 2008). The relative scarcity of Antillean microatolls unfortunately prevented us from finding any records of earthquakes or deformation in the 19th century or earlier—so far the only known instance comes from an exceptionally long-lived specimen on Martinique Island (Weil-Accardo et al., 2016a). Nevertheless, by persistent searching we were able to obtain a spatially distributed set of coral records that document 20th-century deformation.

We collected cross sections from living microatolls at nine sites throughout the Antigua-Barbuda-Guadeloupe region and observed coral morphology at three other sites including one on Anguilla Island (Fig. 4). We obtained an x-ray image of each microatoll

cross section and assigned an age to every annual band by counting back high-low density couplets from the living surface of the colony. Maps of each site and photographs and cross-sections of each coral slice appear in supplementary Figures S1–S19. Growth histories of all the slabs we collected are shown in Fig. 5. Each of these corals hit HLS at numerous points throughout their lives, as indicated by instances where the upper few mm or cm of the colony died. These "die-downs" indicate that the upper part of the coral experienced sufficient duration or intensity of exposure to kill the polyps.

While die-downs on an individual coral or at a single site may be caused by a variety of local environmental factors, contemporaneous die-downs affecting multiple corals at different sites are presumably due to regional environmental events. In Sumatra, non-tectonic regional coral die-downs are dominantly caused by large, prolonged negative sea level anomalies (SLA), up to 30 cm below mean sea level (MSL), that occur during strong Indian Ocean Dipole (IOD) events (Philibosian et al., 2014). The Caribbean does not experience such extreme oceanographic fluctuations, but it is still possible that regional die-downs are linked to SLA. Mean sea surface height (SSH) in the Lesser Antilles typically varies by ~25 cm annually due to the seasonal steric cycle (Alvera-Azcárate et al., 2009). Thus, annual negative sea level anomalies are typically 5–10 cm below MSL, but more rarely drop as low as 25 cm below MSL. Regional coral bleaching events may also cause synchronous die-downs. Additionally, unlike Sumatra, the Caribbean experiences hurricanes which can impact coral growth. In our coral records we observe synchronous regional die-downs as well as isolated local die-downs, but we defer the full exploration of the likely causes to a future paper. Regardless of the precise causes, the recorded series of die-downs indicates that the growth of each of our specimens was repeatedly limited by RSL and therefore can be expected to accurately record RSL trends.

For each of our specimens, we calculate submergence or emergence rates by fitting a line through the highest level of growth (HLG) points immediately prior to die-downs, as these provide the best estimate of HLS (Meltzner et al., 2010). These rates (with 95% confidence interval uncertainties) are shown as trend lines on Fig. 5 and are compiled in Table 1, ordered from northwest to southeast. Corals that are submerging rapidly do not grow fast enough to reach sea level in most years and therefore naturally hit HLS less often, with the unfortunate consequence that higher submergence rates are less well constrained. Uncertainties are conservatively estimated using the full range of plausible HLS variation for corals with few die-downs and for sites where microatolls were observed but not sampled.

The ~1 cm/yr spread in observed submergence/emergence rates is an order of magnitude larger than the expected maximum variability in 20th-century barystatic sea-level change across the region (Weil-Accardo et al., 2016a). Therefore, the bulk of the observed subsidence and emergence is attributed to tectonic land-level change (though the obtained deformation rates must still be adjusted for non-tectonic sea-level change). Further, the various upper plate faults in the region typically have slip rates on the order of 1 mm/yr or less (Feuillet et al., 2004, 2011; Leclerc et al., 2016), again too slow to explain the observed variability. Given the tectonic setting, the process that is most likely responsible for the observed magnitude and broad distribution of deformation is coupling variability on the subduction interface.

4. Discussion and models of subduction interface locking

4.1. Forward models of megathrust coupling

By plotting the uplift and subsidence rates along a profile perpendicular to the subduction front, we can observe the broader
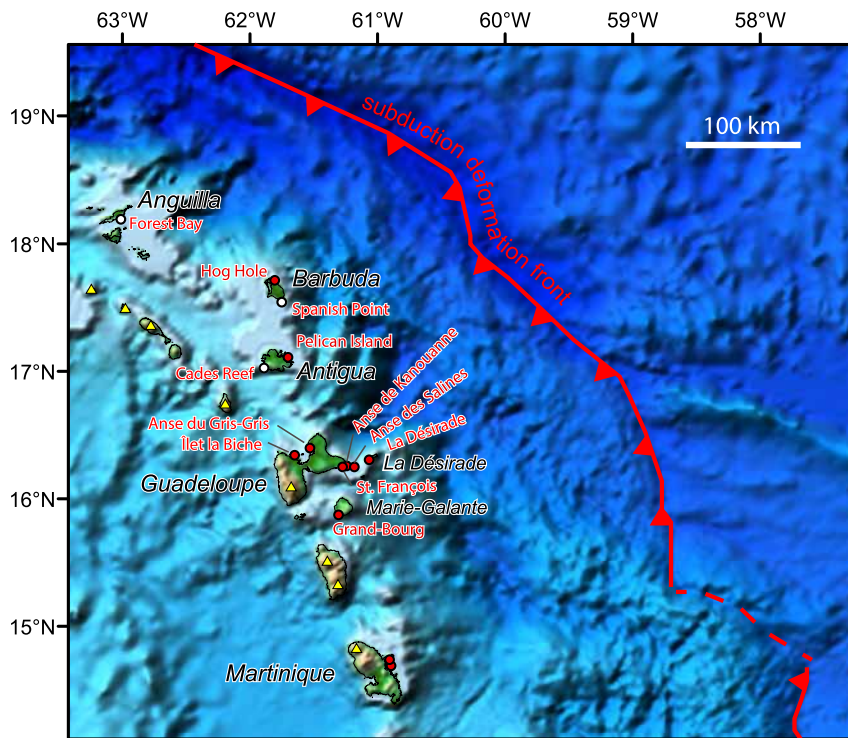
Fig. 4. Regional map of the northern Lesser Antilles with names of major islands and sites where coral slabs were collected (red circles) or coral morphology was observed (white circles). Details of the Martinique sites were presented by Weil-Accardo et al. (2016a). Arc volcanoes are indicated by yellow triangles.

Table 1
Summary of Microatoll Observations.

Latitude	Longitude	Site Name	Island	Year Sampled	Site Code[a]	Emergence Rate[b] (mm/yr)		Uplift Rate[c] (mm/yr)		Time Interval	Duration (yr)
18.195	-63.042	Forest Bay	Anguilla	2014		-2.5	± 3	-1.4	± 3.1	~1950–2014	~60
17.710	-61.801	Hog Hole	Barbuda	2013	HOG	-5.7	± 2	-4.6	± 2.2	1952–2005	53
17.544	-61.733	Spanish Point	Barbuda	2013		-6	± 3	-4.9	± 3.1	~1950–2013	~60
17.106	-61.700	Pelican Island[d]	Antigua	2013	PEL	-9.0	± 2.5	-7.9	± 2.6	1937–1978	41
17.106	-61.700	Pelican Island[d]	Antigua	2013	PEL	-1.4	± 1.2	-0.3	± 1.4	1978–2013	35
17.007	-61.863	Cades Reef	Antigua	2013		0	± 3	1.1	± 3.1	~1950–2013	~60
16.395	-61.526	Anse Gris-Gris	Guadeloupe	2013	AGG	-7.2	± 2.9	-6.1	± 3.0	1941–2007	66
16.338	-61.647	Îlet La Biche	Guadeloupe	2013	BIC	-7	± 3	-5.9	± 3.1	1990–2007	27
16.303	-61.063	La Désirade	La Désirade	2014	DES	-9	± 2	-7.9	± 2.2	1987–2007	30
16.254	-61.241	Anse de Kanouanne	Guadeloupe	2014	KAN	1.0	± 1.2	2.1	± 1.4	1987–2014	37
16.248	-61.268	St. François[e]	Guadeloupe	2011	SFR	-3.3	± 0.6	-2.2	± 1.0	1940–2011	71
16.248	-61.178	Anse des Salines	Guadeloupe	2014	SAL	-3.2	± 0.5	-2.1	± 0.9	1927–2009	82
15.872	-61.302	Grand-Bourg	Marie-Galante	2014	GRB	-1.8	± 0.9	-0.7	± 1.2	1920–2005	85
14.7	-60.9	Robert & Galion Bays[f]	Martinique			-2.4	± 1.0	-1.3	± 1.3	1895–2008	113

[a] Codes were assigned to sites where coral slabs were collected.
[b] Rate uncertainties in italics are estimated (when data points are insufficient to calculate a formal uncertainty).
[c] Corrected for 1.1 ± 0.8 mm/yr of regional 20th-century sea-level rise estimated by Weil-Accardo et al. (2016a).
[d] Rates are calculated separately for the pre- and post-1978 time periods at Pelican Island.
[e] Data originally presented by Weil-Accardo (2014).
[f] Combined from three neighboring sites detailed by Weil-Accardo et al. (2016a).

pattern of deformation and estimate the extent of megathrust coupling that would be required to produce the observed signal. To obtain vertical deformation rates, we correct the submergence and emergence rates for the 1.1 ± 0.8 mm/yr of sea-level rise in the 20th-century Caribbean estimated by Weil-Accardo et al. (2016a). Uncertainties are added in quadrature, assuming that the rates of sea-level rise at each site are normally distributed about the mean. However, the rate of sea-level rise at neighboring sites would be similar, so the relative uncertainties in tectonic deformation rate at neighboring sites are overestimated. Deformation rates are shown alongside the corresponding emergence or submergence rates in Table 1.

We attempt to reproduce the observed vertical deformation rates using simple elastic dislocation models of coupling on the subduction interface. The megathrust geometry is constrained by seismicity and geophysical surveys; we divide sites into four regions and take depth profiles from Laurencin et al. (2018) for Anguilla and from Bie et al. (2020) for Antigua-Barbuda, Guadeloupe, and Martinique (Fig. 6). We assume steady-state subduction in which all parts of the plate interface slip at the same convergence rate regardless of dip, and we use the full plate convergence rate of 2 cm/yr in all models, although in reality this is a maximum since the convergence becomes more oblique northward toward Anguilla (Fig. 1). We use the Coulomb software package (Lin and
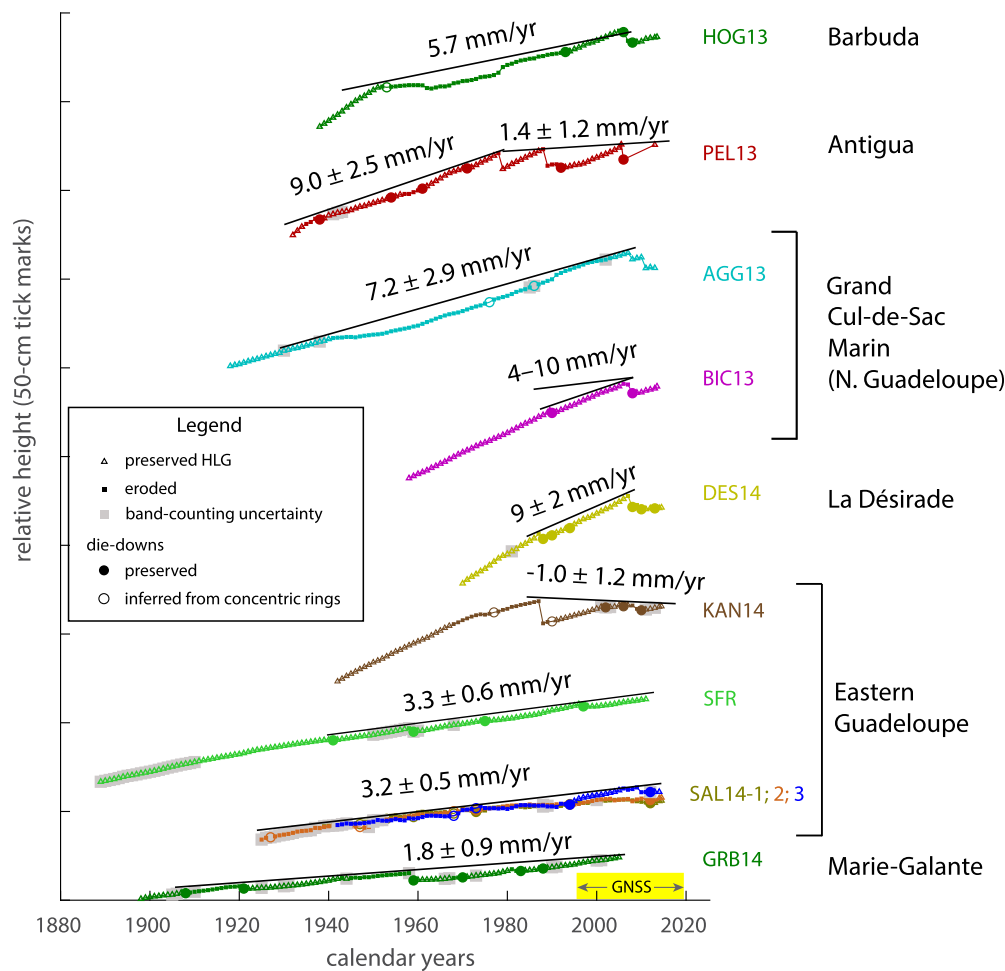
Fig. 5. Growth histories of coral microatolls from eight sites on Barbuda, Antigua, and the Guadeloupe archipelago. Years in which the height of the coral was limited only by coral growth rate are indicated as HLG for highest level of growth. Estimated submergence (positive) or emergence (negative) rates are shown by black trend lines. Rate for SAL was estimated from the best-preserved sections of three slabs; see Figure S12. The period during which GNSS data are available is indicated on the time axis.

Stein, 2004; Toda et al., 2005) to produce backslip models (Savage, 1983) in which fully coupled patches on the plate interface are simulated by imposing normal slip at the plate convergence rate of 2 cm/yr. In general, the updip extent of coupling is not constrained by our data and there are tradeoffs between depth and degree of coupling. We present plausible models with full coupling, with the understanding that a variety of more complex models could fit the data equally well.

Our observed vertical deformation rates are plotted in the upper panels of Fig. 7 along with vertical deformation curves produced by our best-fit forward models, with locked patches for these models indicated on the lower panels. The data from Antigua-Barbuda (including the 1978–2013 rate from the PEL site) fall along the expected deformation trend above the down-dip edge of an interseismically locked patch on the megathrust: zero deformation near the volcanic arc increasing toward a small peak of uplift, then larger subsidence nearer to the subduction front (see Fig. 2). These data are fit well by a fully coupled patch between 30 and 55 km depth (AntBar1 model, Fig. 7). To demonstrate that this model provides a significant improvement over a zero-deformation model, we calculate a weighted mean squared error (WMSE) of 1.4 for AntBar1 in contrast to a WMSE of 14.9 for zero deformation.

While only one poorly constrained data point is available for Anguilla, it would be best fit by a coupled patch at similar depth as in AntBar1. However, a different scenario is required for the 1937–1978 portion of the PEL record, which records a faster subsidence rate than the latter half of the record (see Fig. 5). This

transition suggests a change in the location or degree of megathrust coupling. Similar changes in interseismic deformation rate have also been recorded by microatolls above the Sunda megathrust (Meltzner et al., 2015). The faster pre-1978 subsidence rate at the PEL site requires much deeper coupling, down to 80 km (AntBar2 model, Fig. 7), to be fit within uncertainty. As each is tailored to fit a single data point, it is not meaningful to calculate WMSE for the AntBar2 and Anguilla models.

The data from Guadeloupe are somewhat less straightforward to interpret. While most of the data points follow a curve with the expected shape, the amplitudes of the positive and negative extremes over short distances are too high to be fit well. Several points are fit well by a coupled patch between 30 and 70 km depth (Guad1 model, Fig. 7), but uplift at KAN contrasts too sharply with neighboring sites to be fit by the same curve. One possibility is that the KAN site is affected by a shorter-wavelength process such as upper-plate faulting, though the >3 mm/yr difference is difficult to explain with faults that typically have ∼1 mm/yr slip rates (Feuillet et al., 2004). It is also possible that rather than continuous slow emergence, the KAN record actually represents gradual slow submergence (more similar to surrounding sites) punctuated by a sudden ∼10-cm RSL drop in about 1990 (Fig. 5, Fig. S14). The latter event could have been caused by local nontectonic environmental changes at the site, for example due to Hurricane Hugo which struck Guadeloupe in 1989.

A slightly deeper patch between 35 and 80 km (Guad2 model, Fig. 7) comes the closest to fitting all data points other than KAN
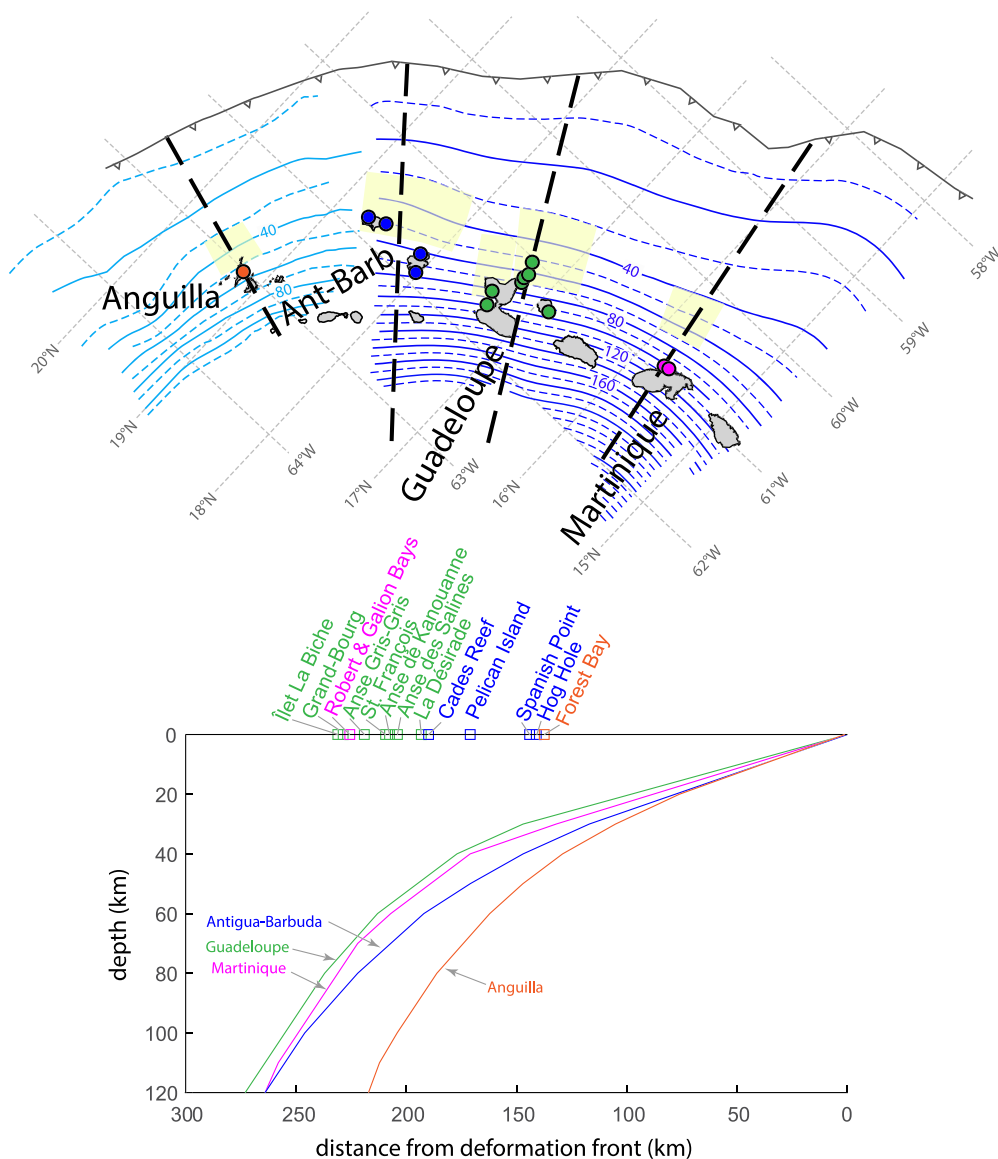
Fig. 6. Megathrust interface geometry used in forward models. (top) Map of the study area with depth contours of the slab interface from Laurencin et al. (2018) for Anguilla and Bie et al. (2020) for other areas. Heavy dashed black lines indicate profiles used in each of four regions. Colored circles show study site locations in each region. Yellow shaded areas indicate inferred locked patches (in general, the updip limit of locking is not constrained). (bottom) Study site locations plotted relative to megathrust geometry in each region.

but passes outside the uncertainty bounds of several. The rapid subsidence at DES and the two points in Grand Cul-de-Sac Marin (GCdSM) can be fit within uncertainty by an even deeper coupled patch (40–90 km, Guad3 model), but this curve cannot simultaneously fit the other data. The GCdSM points are far enough northwestward of the others (25–30 km) that they could be fit independently by varying coupling depth along strike, but DES is too close to the other points for that solution to be plausible. Therefore, DES may also be affected by a shorter-wavelength process. It is also worth noting that the field of corals at Anse du Gris-Gris in GCdSM lies unusually deep, with the living microatoll rims over 50 cm below annual extreme low tide, whereas HLS for these species is typically no more than 20 cm below that level (see Fig. 3). This anomaly suggests that subsidence in recent decades has outpaced the growth rate of the coral, either due to acceleration in subsidence rate or a sudden (perhaps aseismic) subsidence event.

The WMSE values for Guad1, Guad2, and Guad3 are respectively 8.9, 6.8, and 10.6, all of which represent improvements over the 17.3 WMSE of the zero-deformation model. In summary, although

no single simple forward model can fit all the Guadeloupe data, the overall pattern and rates of deformation are generally consistent with coupling between 30 and 90 km on the subduction interface. A more complex model varying the spatial extent and degree of coupling may produce a better fit to the data. The single data point on Martinique is reproduced by a coupled patch between 40 and 70 km depth, intermediate between the Guad1 and Guad2 models (Fig. 7). This is very similar to the estimate of coupling between 30 and 60 km depth inferred by Weil-Accardo et al. (2016a) to explain the same Martinique data using a slightly different elastic model.

4.2. Other evidence for a deep seismogenic zone

While seismogenic zones extending below the overriding plate Moho (∼30 km depth for the Lesser Antilles) might be considered unusual or unlikely, instrumentally recorded seismicity supports this interpretation for the Lesser Antilles. Paulatto et al. (2017) noted M5 thrust events on or near the Lesser Antilles plate inter-
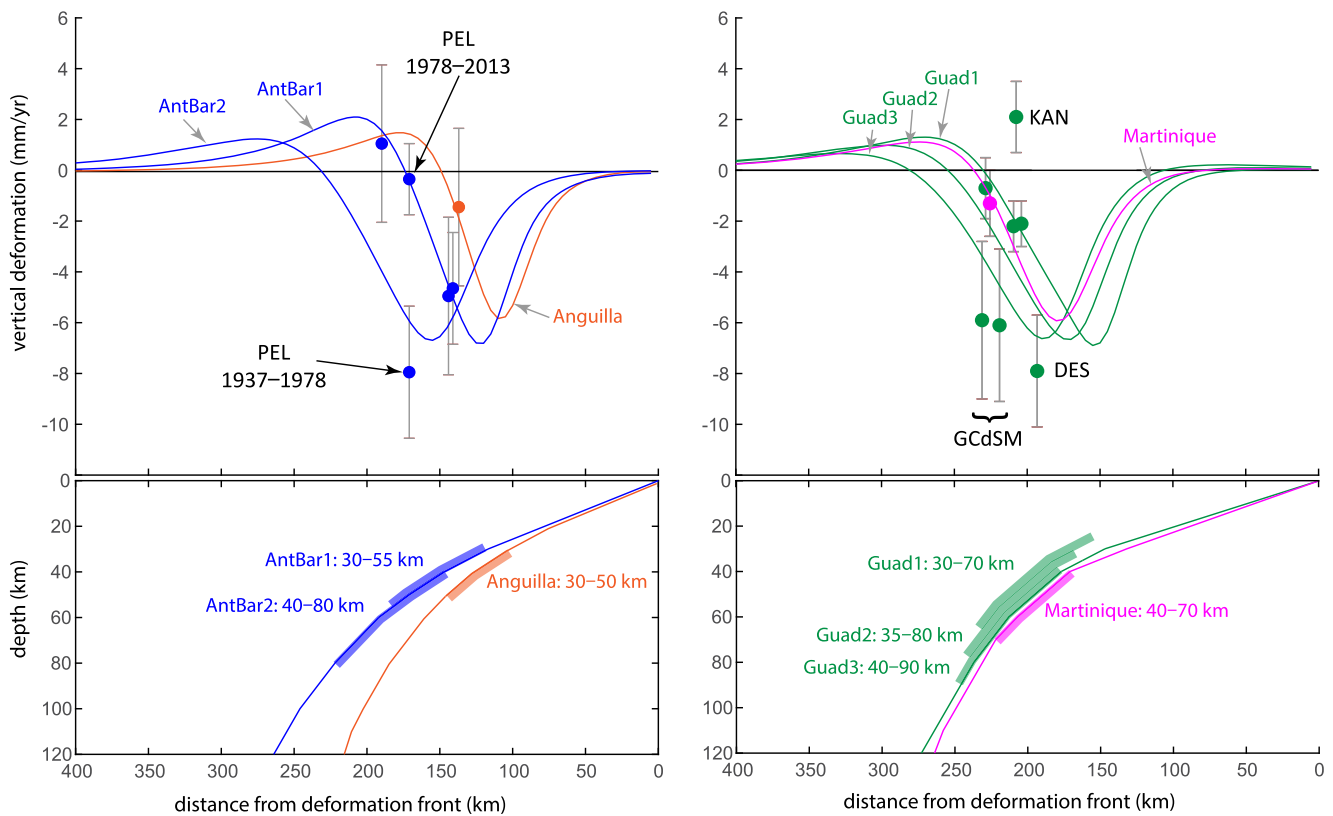
Fig. 7. Forward models of interseismic coupling that best fit microatoll-based vertical deformation rates. Each indicated patch on the plate interface is fully coupled, modeled as back-slipping at the full plate rate of 2 cm/yr. In Antigua-Barbuda, deeper locking is required to fit the faster PEL subsidence rate in the mid-20th century. In Guadeloupe, the uplift at KAN contrasts too sharply with neighboring sites to be fit by the same curve; it may have been affected by a shorter-wavelength deformation process or a site-specific event. The rapid subsidence at DES and in Grand Cul-de-Sac Marin (GCdSM) would require very deep locking to fit even the upper part of their uncertainty ranges.

face between 40 and 50 km depth which are similar to repeating earthquakes associated with the down-dip limit of the seismogenic zone observed along the Japan trench. These events may be generated at the boundaries of locked asperities. Based on the presence of seismicity in the mantle wedge corner and thrust events deep on the megathrust interface, Bie et al. (2020) suggested that the seismogenic zone extends to ∼65 km depth. Furthermore, a small sudden submergence recorded by microatolls suggests that one of the largest instrumentally recorded earthquakes in the region, the 1946 Martinique earthquake (M 6–7), occurred on or near the plate interface below the mantle wedge (Weil-Accardo et al., 2016a). Interestingly, an ongoing cluster of interplate seismicity is located in the estimated rupture area of the 1839 earthquake east of Martinique, and over time has exhibited a deepening trend with events now occurring down to 65 km depth (Corbeau et al., 2021). This migration of seismicity potentially signals a change in extent of coupling on the plate interface, which is a possible precursor for a large seismic or slow-slip event.

4.3. Comparison with GNSS-based deformation studies

4.3.1. Horizontal component

The only previous estimates of coupling on the Lesser Antilles megathrust have been based on deformation over the last few decades recorded by GNSS stations. An early study found up to 50% coupling along the megathrust in much of our study area (Manaker et al., 2008), but more recent estimates suggest little or no coupling except potentially in the very shallow domain, which is unconstrained by island-based data (Symithe et al., 2015; van Rijsingen et al., 2020). This result appears to conflict with our

microatoll-based findings. There are several potential explanations for this discrepancy.

First, because these GNSS-based models used only the horizontal component of the GNSS signal, they are prone to reference frame errors in this oceanic region because the distribution of islands (and therefore stations) is very limited. It is difficult to estimate the Caribbean plate velocity given the dearth of stations in the interior (e.g., van Rijsingen et al., 2020). A miscalculation of the overall Caribbean plate motion could easily cause underestimation of horizontal deformation near the plate boundary, which is the expected signal produced by plate interface coupling.

Another potential reason that our results conflict with Symithe et al. (2015) is that they did not model the megathrust interface below 40 km depth, whereas coupling extends well below that level in each of our models. However, van Rijsingen et al. (2020) use a much more realistic slab interface geometry extending to 100 km depth and maintain the finding of little or no coupling in the range of our proposed locked patches. We note that while coupled patches extending above 40 km depth toward the trench do produce large differentials in horizontal motion that are easily precluded by the GNSS data, if coupling is actually confined below 30 km depth (as it is in our models) the resulting horizontal deformation is relatively small, not exceeding 4 mm/yr (Figure S20). While in reality, pinned coupled patches prevent surrounding (particularly updip) areas of the plate interface from creeping at the full plate rate, this effect decays with distance and models indicate that interseismic creep may approach the plate rate updip of a deep locked patch (e.g., Herman et al., 2018). The small horizontal motions produced by isolated deep coupled patches are plausibly within uncertainty for many stations in the region as reported by Symithe et al. (2015). However, the smaller uncertainties

reported by van Rijsingen et al. (2020) likely preclude horizontal plate boundary deformation >1 mm/yr and are therefore inconsistent with most of our models.

Finally, it is possible that the discrepancy in interplate coupling between GNSS- and microatoll-based models is simply due to the different time periods covered by the data: the GNSS records begin no earlier than 1994, thus spanning a maximum of 25 years (Symithe et al., 2015; van Rijsingen et al., 2020), whereas our microatoll records typically span >30 years and sometimes >100 years (Fig. 5). Although the coral dataset also covers the GNSS period, the rates averaged over many decades may not be accurate for shorter time intervals. The coral records generally do not have enough die-downs to estimate independent rates for the post-1994 period, and therefore the coral records can be considered consistent with little or no coupling in the last decade or two. Decadal-scale variations in the distribution and degree of interplate coupling have been observed in other subduction zones (e.g., Meltzner et al., 2015) and inferred in the past from the longest continuous Antillean coral record, from Martinique (Weil-Accardo et al., 2016a), so this is a plausible scenario. If that is the case, the microatoll-based models provide the more accurate representation of the long-term coupling state and seismic potential of the Lesser Antilles megathrust, whereas the GNSS-based models may represent more transient recent conditions.

4.3.2. Vertical component

The vertical component of GNSS data, more directly comparable to microatoll data, has received relatively little analysis in this region since uncertainties are typically much larger than for the horizontal component. One of the few such studies examined vertical velocities in the Guadeloupe archipelago and on Martinique Island using data recorded between 2001 and 2019, revealing subsidence at most stations at rates typically of a few mm/yr (Sakic et al., 2020). The overall pattern across both islands is of slow subsidence (~1 mm/yr) towards the east increasing to ~5 mm/yr towards the west in the volcanic arc.

While the GNSS vertical deformation rates are of the same order of magnitude and sign as those derived from microatolls, more detailed comparison produces mixed results. There are three locations where GNSS sites and microatoll sites are sufficiently co-located to compare rates: the central-east coast of Martinique, Grand-Bourg on Marie-Galante Island, and La Désirade Island. The first two indeed yield similar results: the ILAM GNSS site and our microatolls from Martinique both exhibit subsidence rates of ~1 mm/yr, as do the MAGA GNSS site and our site GRB near Grand-Bourg. However, GNSS sites on La Désirade island are subsiding at rates of at most 1 mm/yr, whereas the microatoll there suggests 8 mm/yr of subsidence. Since the sites are not exactly co-located it is possible, though unlikely, that the latter discrepancy is due to crustal normal faults running between the sites. Indeed, it is difficult to conceive of a scenario in which a fault with an ~1 mm/yr slip rate could produce a >5 mm/yr difference in deformation between these sites.

The vertical GNSS data express a westward tilt across the islands, from ~1 mm/yr of subsidence on the easternmost points to ~5 mm/yr of subsidence in the volcanic arc (Sakic et al., 2020). While megathrust coupling would not be expected to produce such significant subsidence in the volcanic arc, a similar pattern of westward tilting has been identified in the longer-term uplift and subsidence of Pleistocene coral platforms across the Guadeloupe archipelago (Feuillet et al., 2004; Leclerc et al., 2014; Leclerc and Feuillet, 2019) which likely reflects a broader-scale subduction process such as the effect of a ridge on the subducting plate. Long-term subsidence of the volcanic arc is also demonstrated by the now-submerged Kahouanne Seamounts northwest of Guadeloupe (Carey et al., 2020). However, the deformation rates de-

rived in these geologic studies are much lower (<1 mm/yr) than those evident in the GNSS data, and while the long-term tilting of Guadeloupe is in the same direction, the dominant long-term geologic signal is of uplift (Feuillet et al., 2004) rather than the subsidence observed in the GNSS data (Sakic et al., 2020). Therefore, the origin of the very strong subsidence signal in the GNSS data is unclear. In any case, it is unknown whether the microatoll data match the overall spatial pattern of westward tilting observed in the GNSS data since we have not collected microatolls from the western parts of the islands, within the volcanic arc.

The GNSS-based vertical deformation rates may have additional uncertainties that could encompass apparent discrepancies with microatoll-based rates. Sakic et al. (2020) found that while the overall pattern remained unchanged, substantial differences in magnitude (and even reversal of sign) at some sites were produced when analyzed using two different geodetic software packages. Furthermore, rates at some neighboring GNSS sites are unreasonably different, suggesting the uncertainties may be overall underestimated. Finally, as with the horizontal GNSS data, the vertical GNSS rates are measured over a much shorter time period than the microatoll-based rates and could differ simply for that reason.

4.3.3. Summary and potential limitations

Respective interpretations of our microatoll data and horizontal GNSS data imply disparate megathrust coupling regimes. Direct comparison between microatoll-based and GNSS-based vertical deformation rates reveals mixed consistency. While we discuss above various potential inaccuracies in the GNSS data that may be responsible for these discrepancies, it is of course also possible that some discrepancies can be attributed to inaccuracies in the microatoll-derived deformation rates. For any one microatoll study site, it is possible to argue that the vertical deformation rate is incorrect due to the sampled specimen being anomalous, site conditions producing growth unrepresentative of relative sea level, etc. This may indeed be the case for a few sites such as DES, which has an inherently more uncertain fast subsidence rate, has only two specimens observed rather than a large microatoll field, and is difficult to reconcile both with other nearby microatoll sites and with local GNSS data. However, it is very unlikely that all of our observations result from site-specific anomalies.

5. Conclusions

Our study estimates 20th-century vertical deformation rates from coral microatolls throughout the northern Lesser Antilles forearc, with a total variability of ~1 cm/yr. The data are largely consistent with deformation patterns expected from plate interface coupling between 30 and 70 km depth, though some sites require the contribution of other processes or effects such as crustal faulting or local environmental changes. Our results are in contrast to those based on horizontal GNSS data that imply little to no coupling on the plate interface (van Rijsingen et al., 2020). If both microatoll and GNSS datasets and interpretations are accurate, the most likely explanation for the difference is a change in megathrust coupling toward the end of the 20th century. Regardless of the details, the major result of our study is the evidence of strain accumulation on the Lesser Antilles megathrust throughout the majority of the 20th century, building up to a potential future large earthquake.

CRediT authorship contribution statement

Belle Philibosian: Conceptualization, Formal analysis, Funding acquisition, Investigation, Methodology, Writing – original draft. **Nathalie Feuillet:** Conceptualization, Funding acquisition, Investigation, Methodology, Project administration, Supervision, Writing

– review & editing. **Jennifer Weil-Accardo:** Formal analysis, Investigation, Methodology, Writing – original draft. **Eric Jacques:** Investigation, Writing – review & editing. **Abel Guihou:** Investigation, Writing – review & editing. **Anne-Sophie Mériaux:** Investigation, Writing – review & editing. **André Anglade:** Investigation. **Jean-Marie Saurel:** Investigation. **Sébastien Deroussi:** Investigation.

Declaration of competing interest

The authors declare that they have no known competing financial interests or personal relationships that could have appeared to influence the work reported in this paper.

Appendix A. Supplementary material

Supplementary material related to this article can be found online at https://doi.org/10.1016/j.epsl.2021.117343.

References

Agnew, D.C., 2012. SPOTL: Some Programs for Ocean-Tide Loading. Technical Report. Scripps Institution of Oceanography.

Alvera-Azcárate, A., Barth, A., Weisberg, R.H., 2009. The surface circulation of the Caribbean Sea and the Gulf of Mexico as inferred from satellite altimetry. J. Phys. Oceanogr. 39, 640–657. https://doi.org/10.1175/2008JPO3765.1.

Bie, L., et al., 2020. Along-arc heterogeneity in local seismicity across the Lesser Antilles subduction zone from a dense ocean-bottom seismometer network. Seismol. Res. Lett. 91 (1), 237–247. https://doi.org/10.1785/0220190147.

Briggs, R.W., Sieh, K., Amidon, W.H., Galetzka, J., Prayudi, D., Suprihanto, I., Sastra, N., Suwargadi, B., Natawidjaja, D., Farr, T.G., 2008. Persistent elastic behavior above a megathrust rupture patch: Nias island, West Sumatra. J. Geophys. Res. 113, B12406. https://doi.org/10.1029/2008JB005684.

Budd, A.F., Fukami, H., Smith, N.D., Knowlton, N., 2012. Taxonomic classification of the reef coral family Mussidae (Cnidaria: Anthozoa: Scleractinia). Zool. J. Linn. Soc. 166 (3), 465–529. https://doi.org/10.1111/j.1096-3642.2012.00855.x.

Carey, S., et al., 2020. The polygenetic Kahouanne Seamounts in the northern Lesser Antilles island arc: evidence for large-scale volcanic island subsidence. Mar. Geol. 419, 106046. https://doi.org/10.1016/j.margeo.2019.106046.

Corbeau, J., Gonzalez, O., Feuillet, N., Lejeune, A.-M., Fontaine, F.R., Clouard, V., Saurel, J.-M., the OVSM team, 2021. A significant increase in interplate seismicity near major historical earthquakes offshore Martinique (FWI). Bull. Seismol. Soc. Am. https://doi.org/10.1785/0120200377.

Egbert, G.D., Erofeeva, S.Y., 2002. Efficient inverse modeling of barotropic ocean tides. J. Atmos. Ocean. Technol. 19, 183–204.

Feuillet, N., Tapponnier, P., Manighetti, I., 2004. Differential uplift and tilt of Pleistocene reef platforms and Quaternary slip rate on the Morne-Piton normal fault (Guadeloupe, French West Indies). J. Geophys. Res. 109, B02404. https://doi.org/10.1029/2003JB002496.

Feuillet, N., Beauducel, F., Tapponnier, P., 2011. Tectonic context of moderate to large historical earthquakes in the Lesser Antilles and mechanical coupling with volcanoes. J. Geophys. Res. 116, B10308. https://doi.org/10.1029/2011JB008443.

Herman, M.W., Furlong, K.P., Govers, R., 2018. The accumulation of slip deficit in subduction zones in the absence of mechanical coupling: implications for the behavior of megathrust earthquakes. J. Geophys. Res., Solid Earth 123, 8260–8278. https://doi.org/10.1029/2018JB016336.

Hough, S.E., 2013. Missing great earthquakes. J. Geophys. Res. 118 (B3), 1098–1108. https://doi.org/10.1002/jgrb.50083.

Khan, N.S., Ashe, E., Shaw, T.A., Vacchi, M., Walker, J., Peltier, W.R., Kopp, R.E., Horton, B.P., 2015. Holocene relative sea-level changes from near-, intermediate-, and far-field locations. Curr. Clim. Change Rep. 1, 247–262. https://doi.org/10.1007/s40641-015-0029-z.

Khan, N.S., et al., 2017. Drivers of Holocene sea-level change in the Caribbean. Quat. Sci. Rev. 155, 13–36. https://doi.org/10.1016/j.quascirev.2016.08.032.

Laurencin, M., Graindorge, D., Klingelhoefer, F., Marcaillou, B., Evain, M., 2018. Influence of increasing convergence obliquity and shallow slab geometry onto tectonic deformation and seismogenic behavior along the Northern Lesser Antilles zone. Earth Planet. Sci. Lett. 492, 59–72. https://doi.org/10.1016/j.epsl.2018.03.048.

Leclerc, F., et al., 2014. The Holocene drowned reef of Les Saintes plateau as witness of a long-term tectonic subsidence along the Lesser Antilles volcanic arc in Guadeloupe. Mar. Geol. 355, 115–135. https://doi.org/10.1016/j.margeo.2014.05.017.

Leclerc, F., Feuillet, N., Deplus, C., 2016. Interactions between active faulting, volcanism, and sedimentary processes at an island arc: insights from Les Saintes channel, Lesser Antilles arc. Geochem. Geophys. Geosyst. 17 (7), 2781–2802. https://doi.org/10.1002/2016GC006337.

Leclerc, F., Feuillet, N., 2019. Quaternary coral reef complexes as powerful markers of long-term subsidence related to deep processes at subduction zones: insights from Les Saintes (Guadeloupe, French West Indies). Geosphere 15 (4), 983–1007. https://doi.org/10.1130/GES02069.1.

Lin, J., Stein, R.S., 2004. Stress triggering in thrust and subduction earthquakes, and stress interaction between the southern San Andreas and nearby thrust and strike-slip faults. J. Geophys. Res. 109 (B2), B02303. https://doi.org/10.1029/2003JB002607.

Manaker, D.M., Calais, E., Freed, A.M., Ali, S.T., Przybylski, P., Mattioli, G., Jansma, P., Prépetit, C., de Chabalier, J.B., 2008. Interseismic Plate coupling and strain partitioning in the Northeastern Caribbean. Geophys. J. Int. 174 (3), 889–903. https://doi.org/10.1111/j.1365-246X.2008.03819.x.

McCaffrey, R., 2008. Global frequency of magnitude 9 earthquakes. Geology 36 (3), 263–266. https://doi.org/10.1130/G24402A.1.

Meltzner, A.J., Sieh, K., Chiang, H.-W., Shen, C.-C., Suwargadi, B.W., Natawidjaja, D.H., Philibosian, B.E., Briggs, R.W., Galetzka, J., 2010. Coral evidence for earthquake recurrence and an A.D. 1390–1455 cluster at the south end of the 2004 Aceh-Andaman rupture. J. Geophys. Res. 115, B10402. https://doi.org/10.1029/2010JB007499.

Meltzner, A.J., et al., 2015. Time-varying interseismic strain rates and similar seismic ruptures on the Nias–Simeulue patch of the Sunda megathrust. Quat. Sci. Rev. 122, 258–281. https://doi.org/10.1016/j.quascirev.2015.06.003.

Paulatto, M., Laigle, M., Galve, A., Charvis, P., Sapin, M., Bayrakci, G., Evain, M., Kopp, H., 2017. Dehydration of subducting slow-spread oceanic lithosphere in the Lesser Antilles. Nat. Commun. 8. https://doi.org/10.1038/ncomms15980.

Philibosian, B., Sieh, K., Avouac, J.-P., Natawidjaja, D.H., Chiang, H.-W., Wu, C.-C., Perfettini, H., Shen, C.-C., Daryono, M.R., Suwargadi, B.W., 2014. Rupture and

variable coupling behavior of the Mentawai segment of the Sunda megathrust during the supercycle culmination of 1797 to 1833. J. Geophys. Res. 119. https://doi.org/10.1002/2014JB011200.

Philibosian, B., et al., 2017. Earthquake supercycles on the Mentawai segment of the Sunda megathrust in the seventeenth century and earlier. J. Geophys. Res., Solid Earth 122 (1), 642–676. https://doi.org/10.1002/2016JB013560.

Sakic, P., Männel, B., Bradke, M., Ballu, V., de Chabalier, J.-B., Lemarchand, A., 2020. Estimation of Lesser Antilles vertical velocity fields using a GNSS-PPP software comparison. In: International Association of Geodesy Symposia. Springer, Berlin, Heidelberg.

Savage, J.C., 1983. A dislocation model of strain accumulation and release at a subduction zone. J. Geophys. Res. 88, 4983–4996.

Symithe, S., Calais, E., de Chabalier, J.B., Robertson, R., Higgins, M., 2015. Current block motions and strain accumulation on active faults in the Caribbean. J. Geophys. Res., Solid Earth 120 (5), 3748–3774. https://doi.org/10.1002/2014JB011779.

Taylor, F.W., Frohlich, C., Lecolle, J., Strecker, M.R., 1987. Analysis of partially emerged corals and reef terraces in the central Vanuatu Arc; comparison of contemporary coseismic and nonseismic with Quaternary vertical movements. J. Geophys. Res. 92 (B6), 4905–4933. https://doi.org/10.1029/JB092iB06p04905.

Toda, S., Stein, R.S., Richards-Dinger, K., Bozkurt, S., 2005. Forecasting the evolution of seismicity in southern California: animations built on earthquake stress transfer. J. Geophys. Res., Solid Earth 110 (B5), B05S16. https://doi.org/10.1029/2004JB003415.

van Rijsingen, E.M., Calais, E., Jolivet, R., de Chabalier, J.B., Jara, J., Symithe, S., Robertson, R., Ryan, G.A., 2020. Inferring interseismic coupling along the Lesser Antilles arc: a Bayesian approach. J. Geophys. Res., Solid Earth 126 (2), e2020JB020677. https://doi.org/10.1029/2020JB020677.

Weil-Accardo, J., 2014. Variations séculaires du niveau marin relatif liées au fonctionnement du méga chevauchement et au climat dans les Antilles: Apport des microatolls coralliens. Ph.D. thesis. Institut de Physique du Globe de Paris.

Weil-Accardo, J., Feuillet, N., Jacques, E., Deschamps, P., Beauducel, F., Cabioch, G., Tapponnier, P., Saurel, J.M., Galetzka, J., 2016a. Two hundred thirty years of relative sea level changes due to climate and megathrust tectonics recorded in coral microatolls of Martinique (French West Indies). J. Geophys. Res., Solid Earth 121 (4), 2873–2903. https://doi.org/10.1002/2015JB012406.

Weil-Accardo, J., Feuillet, N., Jacques, E., Deschamps, P., Saurel, J.-M., Thirumalai, K., Demeza, S., Anglade, D., 2016b. Relative sea-level changes during the last century recorded by coral microatolls in Belloc, Haiti. Glob. Planet. Change 139 (), 1–14. https://doi.org/10.1016/j.gloplacha.2015.12.019.